

# Complex Dynamic Phenomena in a Low-order Model of Non-basal Testosterone Regulation

Zhanybai T. Zhusubaliyev, Alexander N. Churilov and Alexander Medvedev

**Abstract**—Complex nonlinear dynamics in a recent mathematical model of non-basal testosterone regulation are investigated. In agreement with biological evidence, the pulsatile (non-basal) secretion of testosterone is modeled by frequency and amplitude modulated feedback. It is shown that, in addition to already known periodic solutions with one and two pulses in the least period of the closed-loop solution, cycles of higher periodicity and chaos are present in the model in hand. The broad range of exhibited dynamical behaviors makes the model highly promising in model-based signal processing of hormone data.

## I. INTRODUCTION

Hormones are signaling molecules, acting as chemical messengers from one cell (or a group of cells) to another, and are produced by nearly every organ and tissue type in a multi-cellular organism. Hormones are secreted mainly in endocrine glands directly in the blood stream. Hormonal (endocrine) regulation is seen as a complex dynamical biological system where hormones, often represented as their serum concentrations, interact via numerous feedback and feedforward relationships, see [1] and [2].

Endocrine glands secrete their product (hormones) either in continuous (basal) or pulsatile (non-basal) manner. The pulsatile hormone secretion generally stems from the pulse dynamics of neurons. Hormone concentration pulses are modulated in amplitude and frequency [3], [4] with both characteristics imparting biological effect. Within a feedback construct, pulsatile hormone secretion gives rise to a dynamical system where amplitude and frequency modulation is employed to control concentration of other hormones, typically in order to induce sustained oscillations in the closed-loop system.

Mathematical models of endocrine systems are mostly intended as quantitative representations of currently available medical and biological knowledge and designed to perform experiments *in silico*. For instance, a recently devised mathematical model of the human menstrual cycle [5] consists of 43 ordinary differential equations with 191 parameters. To enable mathematical analysis, coarse-grained low-order models of endocrine systems are rather needed. Another driving factor to this end is the development of model-based

signal processing and control algorithms for endocrine application, e.g. the artificial pancreas [6] or state observers for the reconstruction of inaccessible for measurement hormone concentrations [7].

In endocrinology, a classical example of a low-order model is the Smith model of testosterone regulation [1]. Apparently, this model, even augmented with a delayed feedback, is proven in [8] to possess a unique globally asymptotically stable equilibrium point, which property contradicts the pulsatile nature of non-basal endocrine regulation. A limited repertoire of dynamical behaviors is an inherent limitation of smooth continuous low-order models. However, under piecewise linear (affine) nonlinearities in the feedback path of the Smith model, complex dynamical phenomena such as cycles of higher periodicity and chaos arise in the system [9]–[11]. Similar richness of dynamics is observed in another detailed simulation model of the female menstrual cycle [12] where amplitude and frequency modulation as well as feedback time delays are combined with high-order Hill functions. In this case, it is difficult to discriminate between the contributions of different dynamical components to the resulting nonlinear phenomena.

Periodic solutions in a low-order model of non-basal (pulsatile) testosterone regulation suggested in [13] have been recently analyzed in [14]. The model is shown to possess sustained periodic oscillations with one and two pulses in the least period of a closed-loop system solution that is a clear improvement in comparison with the classical Smith model. A more comprehensive search for other dynamical behaviors of this model was though out of scope there.

Interestingly enough, some recent findings emanating from research based on clinical data suggest that chaotic phenomena indeed occur in endocrine systems. A nonlinear dynamics analysis of several thousands of menstrual cycles in [15] provided significant evidence that the menstrual cycle is the result of chaos. Similarly, deterministic chaos was strongly indicated in measured with high resolution (2 min. sampling) pulsatile secretion of parathyroid hormone [16].

The role of chaos in endocrine systems remains for the time being a debatable issue. The classical point of view implicating chaos in disease [9] seems to drift towards appreciating it as a normal “broadband” and “information-rich” condition [16]. In any case, the occurrence of chaos in a mathematical model of an endocrine system indicates the dynamical richness of the model and its ability to produce trajectories highly reminding actual measured hormone concentration data.

The present paper takes further the earlier presented analysis of a hybrid model for non-basal testosterone secretion [14] and shows that solutions of higher periodicity

Zh. Zhusubaliyev is with the Dept. of Computer Science, South West State University, 50 Years of October Str., 94, 305040, Kursk, Russia, zhanybai@hotmail.com

A. Churilov is with the Faculty of Mathematics and Mechanics, St. Petersburg State University, Universitetsky av. 28, Peterhof, 198504, St. Petersburg, Russia, a\_churilov@mail.ru

A. Medvedev is with Information Technology, Uppsala University, SE-751 05 Uppsala, Sweden, alexander.medvedev@it.uu.se

A. Churilov was supported by the Russian Foundation for Basic Research, Grant 10-01-00107-a. A. Medvedev was in part financed by the European Research Council, Advanced Grant 247035 (SysTEAM).

and chaos occur under pulse-modulated feedback in a third-order smooth model of hormone kinetics. It demonstrates that the considered hybrid model can display a great variety of nonlinear dynamical phenomena, including finite and infinite sequences of direct and reverse period-doubling cascades as well as a period-doubling transition to chaos. Bifurcation analysis proves the model to be monostable with bifurcation curves in the form of closed contours.

The paper is organized as follows. First a brief description of pulsatile testosterone secretion in the male, together with its mathematical formulation as a pulse modulated feedback system, are provided. Then, a bifurcation analysis of the model for the special case of a second-order Hill function as the modulation function is carried out. Further, the changes in dynamical phenomena arising for higher-order Hill functions are considered.

## II. SYSTEM DESCRIPTION

In the endocrine regulation of testosterone (Te) in the male, an essential role is played by the luteinizing hormone (LH) and gonadotropin-releasing hormone (GnRH). While Te is produced in testes, LH and GnRH are secreted in different parts of the brain — hypophysis (pituitary gland) and hypothalamus, respectively.

The pulsatile secretion of GnRH stimulates the secretion of LH, which, in turn, stimulates the production of Te, while Te inhibits the secretion of GnRH and LH [17]. Thus, there arises an endocrine feedback loop GnRH-LH-Te with pulse modulated control through the pulsatile secretion of GnRH. Notice that the pulsatile character of the GnRH release is a necessary attribute of the endocrine system since a continuous administration of GnRH would not stimulate the production of LH [18].

Experimental studies reveal that concentrations of Te and LH in the adult male exhibit oscillative behavior and their exact signal forms depend on the individual. As for direct measurements of GnRH in the human, they are difficult to implement due to ethical reasons. Oscillations in hormone concentrations are of a broad spectrum. Ultradian harmonics with a period of 1 – 3 h, depending on the individual, are present and a circadian rhythm of 24 h is clearly observed.

In order to explicitly describe the pulsatile mechanism of non-basal secretion of Te, the classical Smith model [1] was in [14] modified by the introduction of a frequency and amplitude pulse modulated feedback [19]. The resulting system is governed by a system of three coupled ordinary differential equations

$$\dot{x} = Ax + B\xi(t) \quad (1)$$

with

$$\xi(t) = \sum_{k=0}^{\infty} \gamma_k \delta(t - t_k)$$

and

$$x = \begin{bmatrix} x_1 \\ x_2 \\ x_3 \end{bmatrix}, \quad A = \begin{bmatrix} -b_1 & 0 & 0 \\ g_1 & -b_2 & 0 \\ 0 & g_2 & -b_3 \end{bmatrix}, \quad B = \begin{bmatrix} 1 \\ 0 \\ 0 \end{bmatrix}.$$

The concentration of GnRH corresponds to  $x_1$ , the concentrations of LH and Te are given by  $x_2$  and  $x_3$ , respectively.

The positive constants  $b_1, b_2, b_3$  and  $g_1, g_2$  are defined by the kinetics of the involved hormones and  $\delta(\cdot)$  denotes the Dirac function. Notably, none of the biologically meaningful variables in the model above are unbounded and the Dirac functions are simply used for marking the instants of GnRH release.

The pulse firing times  $t_k$  are determined by  $t_{k+1} = t_k + \tau_k$ ,  $\tau_k = \Phi(x_3(t_k))$  and  $\gamma_k = F(x_3(t_k))$ , where

$$\Phi(x_3) = k_1 + k_2 \frac{(x_3/h)^p}{1 + (x_3/h)^p}, \quad F(x_3) = k_3 + \frac{k_4}{1 + (x_3/h)^p}$$

represent frequency and amplitude modulation characteristics, respectively. Here parameters  $k_1, k_2, k_3, k_4, h$  are positive and  $p \geq 1$  is an integer number. The function  $\Phi(\cdot)$  is known as Hill (sigmoidal) function. To keep in touch with the biological nature of the system, the value of  $p$  (Hill function order) should be kept reasonably low. Hill functions of high order behave as a relay and sometimes are used in smooth closed-loop systems to induce oscillations.

Model (1) is a so-called positive system, i.e.  $x_i(t) \geq 0$ ,  $i = 1, 2, 3$ , reflecting the fact that hormone concentrations remain non-negative for  $t \geq 0$  if their initial values are non-negative. It is easily seen that system (1) has no equilibria. Since the impulse frequency and the impulse weights are bounded from above, all the solutions of (1) are bounded. Moreover, as time increases, any solution of (1) enters and stays within a certain bounded region in the phase space and this region does not depend on the initial values.

The period  $T$  of a periodic solution  $X_c(t)$ ,  $X_c(t+T) \equiv X_c(t)$  of dynamical system (1) is equal to the sum of the durations of the time intervals  $\tau_k = t_{k+1} - t_k$

$$T = \sum_{k=0}^{m-1} \tau_k,$$

where  $m$  is the number of impulses during the period  $T$ . Such a solution is termed as  $m$ -cycle. Local stability of an  $m$ -cycle is determined by its multipliers, i.e. by the eigenvalues of the monodromic matrix [20].

## III. BIFURCATION ANALYSIS FOR THE SYSTEM WITH HILL FUNCTIONS OF THE SECOND ORDER

Periodic solutions of hybrid model (1) with one or two pulses of GnRH in the least period, i.e. stable 1-cycles and 2-cycles, were observed and analyzed in [14]. It was also revealed that a 2-cycle arises from a 1-cycle in a period-doubling bifurcation.

In this section the following values of the parameters are assumed:  $b_2 = 0.15$ ,  $b_3 = 0.1$ ,  $g_2 = 1.5$ ,  $k_1 = 40$ ,  $k_2 = 80$ ,  $k_3 = 0.05$ ,  $k_4 = 5$ ,  $h = 2.7$ ,  $p = 2$ . The parameters  $b_i, i = 1, 2, 3$  are defined by the half-life times of the hormones and these values are typically known with higher certainty than the rest of the model parameters. Notice e.g. that the gains  $g_1, g_2$  amplify in (1) the amplitudes of the  $\delta$ -functions of the pulsatile feedback. Since the concentration of GnRH is not available for measurement, absolute values of the gains cannot be uniquely established from observed data. The choice of  $p$  is intentionally low in order to avoid the artifacts produced by the switch-like characteristic of the

high-order Hill functions. The effects of steeper modulation characteristics are studied in next section.

In the following bifurcation analysis  $b_1$  and  $g_1$  are used as bifurcations parameters. Thus,  $b_1$  describes the clearing rate of GnRH while  $g_1$  characterizes the secretion rate of LH stimulated by the concentration of GnRH.

As long as the parameter  $g_1$  is small enough, for any  $b_1$ , system (1) has a single stable 1-cycle. When  $g_1$  is relatively large, the model displays more complicated dynamical phenomena, including a cascade of a finite sequence of direct and reverse period-doubling bifurcations as well as a period-doubling route to chaos.

Fig. 1 shows a chart of dynamical modes in the  $(b_1, g_1)$  parameter plane. Here  $\Pi_i$ ,  $i = 1, 2, 3, 4, 8, 16$  are regions of existence for stable  $i$ -cycles. The domains  $\Pi_{2^j-1}$ ,  $j = 1, 2, \dots$  are separated by period-doubling bifurcation curves  $N_-$ . Transverse to these curves are the curves along which the accumulating period-doubling cascades occur.

The regions of chaotic dynamics  $\Pi_\infty$  are broken up by a variety of different periodic zones, each with its internal bifurcation structure. Only two of them ( $\hat{\Pi}_{10}$  and  $\hat{\Pi}_{12}$ ) are depicted in the Fig. 1. The number of such domains in the parameter plane can be infinite. The domain  $\hat{\Pi}_{10}$  is comprised of a union of the sets  $\Pi_{10 \cdot 2^{i-1}}$ ,  $i = 1, 2, \dots$ :

$$\hat{\Pi}_{10} = \bigcup_{i=0}^{\infty} \Pi_{10 \cdot 2^{i-1}}.$$

where  $\Pi_{10 \cdot 2^{i-1}}$  are domains of existence of locally stable  $10 \cdot 2^{i-1}$ -cycles ( $i = 1, 2, \dots$ ). The boundaries, separating these domains in  $\hat{\Pi}_{10}$ , correspond to period-doubling bifurcation curves. These bifurcation curves accumulate, and there exist transverse directions along which infinite series of period-doubling bifurcations take place. The basic domain  $\Pi_{10}$  is bounded from outside by a saddle-node bifurcation curve in the points of which the 10-cycle is first created. The properties of  $\hat{\Pi}_{12}$  are similar to those of  $\hat{\Pi}_{10}$ .

Moreover, as illustrated in Fig. 2, any domain of stability for  $k \cdot 2^i$ -cycles  $\Pi_{k \cdot 2^i}$  is “embedded” into the  $k \cdot 2^{i-1}$ -cycle window  $\Pi_{k \cdot 2^{i-1}}$ ,  $i = 1, 2, \dots$  and delineated by a closed period-doubling bifurcation curve. Here  $k$  is the period of a basic cycle.

First, examine the transition that occurs as moving along the direction  $A$  in Fig. 1, i.e., while the parameter  $b_1$  increases from 0.003 to 0.045 and the parameter  $g_1$  remains constant at  $g_1 = 0.6$ . This transition is shown in Fig. 3 and corresponds to the domains where an incomplete cascade of period-doubling bifurcations is realized.

At the starting point, i.e., for  $b_1 = 0.003$ , system (1) has a single stable 1-cycle. When  $b_1$  increases, the 1-cycle becomes a saddle and undergoes a supercritical period-doubling bifurcation. This produces a stable 2-cycle. With a further increase in  $b_1$ , the 2-cycle undergoes a new period-doubling bifurcation. To explain the mechanism of a finite sequence of period-doubling bifurcations, consider characteristics of the bifurcational behavior shown in Fig. 3 in more detail.

The variation of the critical multiplier for the 2-cycle is shown in Fig. 4. At the bifurcation point  $b_1 = b_1^L$ , the largest (in absolute value) multiplier  $\rho_1$  of the 2-cycle leaves the unit circle through  $-1$  and the 2-cycle turns into an unstable node.

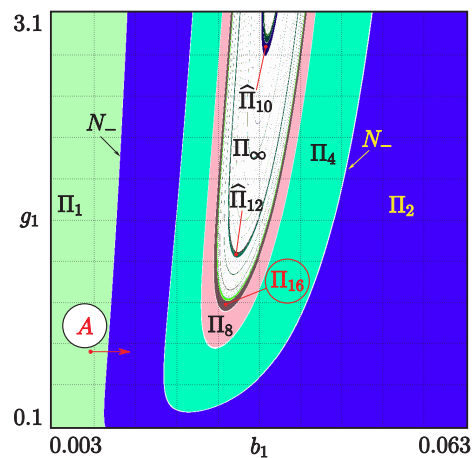


Fig. 1. Chart of dynamical modes in the  $(b_1, g_1)$  parameter plane for  $p = 2$ .  $\Pi_i$ ,  $i = 1, 2, 4, 8, 16$  are the domains of stability for the  $i$ -cycles and  $\Pi_\infty$  are the regions of chaotic dynamics.  $N_-$  is the period-doubling bifurcation curve.

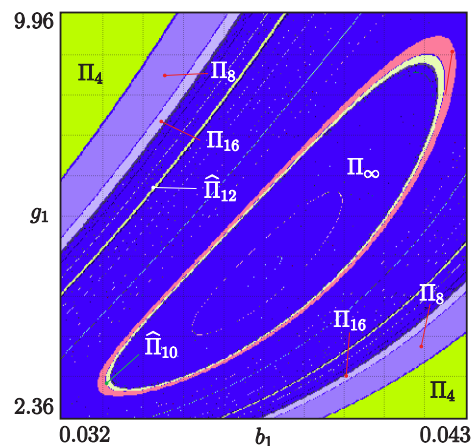


Fig. 2. Part of the chart of the dynamical modes Fig. 1 near the 10-periodic window  $\hat{\Pi}_{10}$ . The periodic window  $\hat{\Pi}_{10}$  is comprised of a union of the sets  $\Pi_{10 \cdot 2^{i-1}}$ ,  $i = 1, 2, \dots, \infty$ , where  $\Pi_{10 \cdot 2^{i-1}}$  are domains of existence of locally stable  $10 \cdot 2^{i-1}$ -cycles ( $i = 1, 2, \dots$ ). Each domain of stability for  $10 \cdot 2^i$ -cycle is “embedded” into the region of existence for a stable  $10 \cdot 2^{i-1}$ -cycle, and delineated by a closed period-doubling bifurcation curve.

Figs. 3 and 4 show that the loss of stability for the 2-cycle is accompanied by the soft birth of a stable 4-cycle. When  $b_1$  passes through the value  $b_1 = b_1^R$ , the largest multiplier of the 2-cycle enters the unit circle through  $-1$ , and the 2-cycle becomes stable again.

To complete the discussion of the system dynamics for  $p = 2$ , consider Fig. 5 that illustrates a classical period-doubling transition to chaos. Fig. 5 displays the results of a one-dimensional bifurcation scan for  $g_1 = 2.0$  in Fig. 1. As illustrated in Fig. 5, with the increase of  $b_1$ , one can observe an infinite cascade of period doubling bifurcations leading to chaos. Fig. 6 depicts a chaotic attractor for  $g_1 = 2.8$  and  $b_1 = 0.031$ .

#### IV. COMPLEX DYNAMICS IN THE SYSTEM WITH HILL FUNCTIONS OF A HIGHER ORDER

In endocrinology, the order of a Hill function in a mathematical model is typically estimated from data or simply used

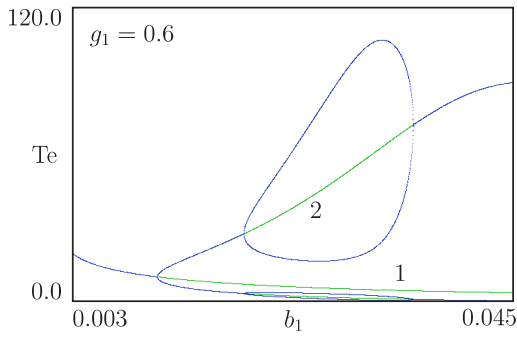


Fig. 3. Bifurcation diagram for  $p = 2$ ,  $g_1 = 0.6$ . Green lines 1 and 2 show unstable 1- and 2-cycles, respectively.

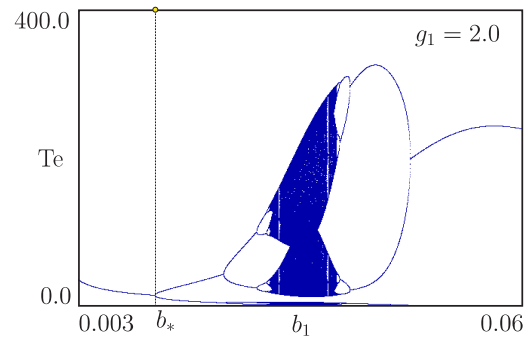


Fig. 5. Transition to chaos through a period-doubling sequence ( $p = 2$ ).

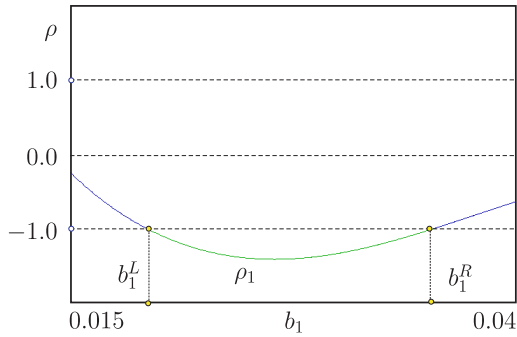


Fig. 4. Multiplier diagram illustrating the direct and reverse period doubling of the 2-cycle (see Fig. 3). Variation of the largest (in absolute value) multiplier of the 2-cycle for  $g_1 = 0.6$ ,  $p = 2$ . With the increase of  $b_1$ , the multiplier of the 2-cycle leaves the unit circle through  $-1$  and the 2-cycle becomes a saddle. As a result, a stable 4-cycle softly arises from the 2-cycle. With the further increase in  $b_1$ , the multiplier of the 2-cycle enters the unit circle through  $-1$ , and the 2-cycle becomes stable again. Here  $b_1^L$  and  $b_1^R$  are the points of the period-doubling bifurcation.

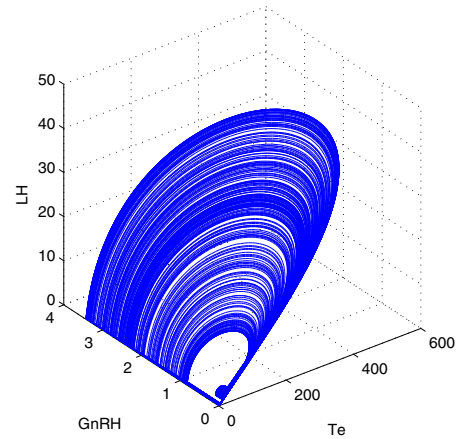


Fig. 6. A chaotic attractor.  $g_1 = 2.8$ ,  $b_1 = 0.031$  and  $p = 2$ .

as a “design” parameter to achieve desired model properties. In this section, changes in dynamical behaviors of system (1) related to the order of the Hill functions are highlighted.

The same model parameter values as previously are utilized below. The difference is that Hill functions of order 4 are considered. Once again, the parameters  $b_1$  and  $g_1$  will be taken as bifurcational parameters.

Fig. 7 shows the chart of dynamical modes (two-parameter bifurcation diagram) in the parameter plane  $(b_1, g_1)$  for  $p = 4$ . When comparing Figs. 1 and 7, one may note that the increase in the Hill function order leads to the appearance of a large periodic window  $\Pi_3 \cup \Pi_6$  with the following peculiarity (in contrast to the case  $p = 2$ ).

As shown in Fig. 7, the domain  $\Pi_3$  of stability for the 3-cycle is bounded from outside by the saddle-node bifurcation curve  $N_+$  and from inside by the period-doubling bifurcation curve  $N_-$ . The domain of 6-cycle dynamics  $\Pi_6$  is “embedded” into the 3-cycle window  $\Pi_3$ , and delineated by a closed period-doubling bifurcation curve. This implies that the 3-cycle undergoes only two period-doubling bifurcations, first a direct bifurcation, and then a reverse one.

To illustrate this peculiarity, Fig. 8 displays a one-dimensional bifurcation diagram obtained by performing a horizontal scan  $B$  in Fig. 7 through the region  $\Pi_3 \cup \Pi_6$  for  $g_1 = 1.0$ . Again, at the starting point, system (1) has a single

stable 1-cycle. As  $b_1$  increases, the stable 1-cycle undergoes a period-doubling bifurcation. This leads to the soft birth of a 2-cycle. With further increase of  $b_1$ , a period-doubling sequence leading to chaotic dynamics occurs. Fig. 9, Fig. 10, and Fig. 11 illustrate the change of the waveform for the concentrations of GnRH, LH and Te during the transition to chaos via the period-doubling sequence. Fig. 12 shows temporal variations of the concentrations of GnRH, LH and Te for the chaotic dynamics.

To further illustrate the above bifurcation behavior, a horizontal scan is performed along the line  $B$  near the periodic window  $\Pi_3 \cup \Pi_6$ . A magnified part of the bifurcation diagram, outlined by the rectangle in Fig. 8, is depicted in Fig. 13. To better illustrate bifurcation transitions, not all branches of the bifurcation diagram are included but only a magnified view of two of three.

At  $b_1 = b_*^+$ , a stable (denoted by the number 1) and a saddle (denoted by the number 2) 3-cycles are born in a saddle-node bifurcation and the system enters the periodic window  $\Pi_3 \cup \Pi_6$ . With further increase in  $b_1$ , namely when  $b_1 = b_*^-$ , the stable 3-cycle undergoes a period-doubling bifurcation. As a result, a stable 6-cycle (denoted by the number 4) softly arises, and the 3-cycle becomes a saddle (denoted by the number 5). When the parameter  $b_1$  passes through the value  $b_1 = b_{**}$ , the saddle 3-cycle again becomes stable as a result of the “reverse” period-doubling bifurcation

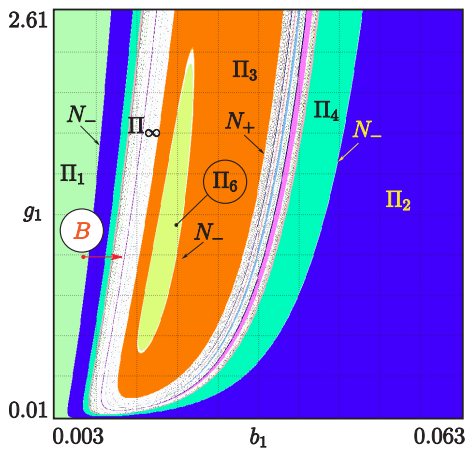


Fig. 7. Chart of dynamical modes in the  $(b_1, g_1)$  parameter plane for  $p = 4$ . Here  $\Pi_i$ ,  $i = 1, 2, 3, 4, 6$  are the domains of stability for the  $i$ -cycles. Regions of chaotic dynamics are indicated by  $\Pi_\infty$ .  $N_-$  is the period-doubling bifurcation curve and  $N_+$  is the saddle-node bifurcation curve.

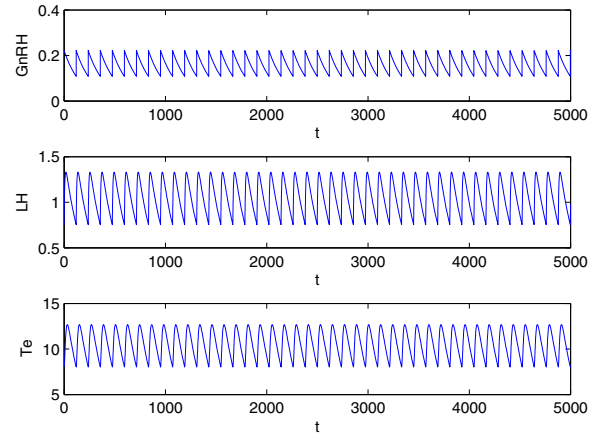


Fig. 9. Temporal variations of concentrations of GnRH, LH and Te for a 1-cycle (see Fig. 8).  $g_1 = 1.0$ ,  $b_1 = 0.006$  and  $p = 4$ .

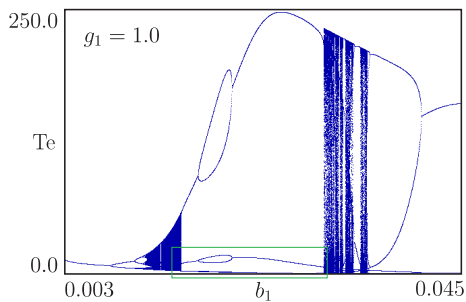


Fig. 8. Transition to chaos through a period-doubling sequence. Bifurcation diagram for  $g_1 = 1.0$  and  $p = 4$ .

(the largest (in absolute value) multiplier of the 3-cycle enters the unit circle through  $-1$ ).

Finally, when crossing the saddle-node bifurcation curve  $N_+$  (see Fig. 7) with increasing  $b_1$  along the direction  $B$ , the stable node 3-cycle (denoted by the number 1) merges with the saddle 3-cycle (denoted by the number 2) and disappears. This leads to an abrupt transition from periodic to chaotic oscillations.

## V. CONCLUSIONS

An earlier proposed parsimonious impulsive model of non-basal feedback hormone regulation is demonstrated to exhibit a wide range of complex dynamical behaviors. In agreement with previous research regarding pulse-modulated mathematical models of non-basal Te regulation, a regular periodic mode with one or two impulses of GnRH in the least period is observed for the main part of the parameter domain. However, there also exist parameter regions where cycles of higher periodicity and deterministic chaos are revealed.

The regions of chaotic dynamics are broken up by a variety of different periodic windows, each with its internal bifurcation structure. The periodic windows are located everywhere dense in the parameter plane, which observation is in line with the lack of equilibria in the system. It appears that each  $k$ -periodic window  $\hat{\Pi}_k$  is comprised of

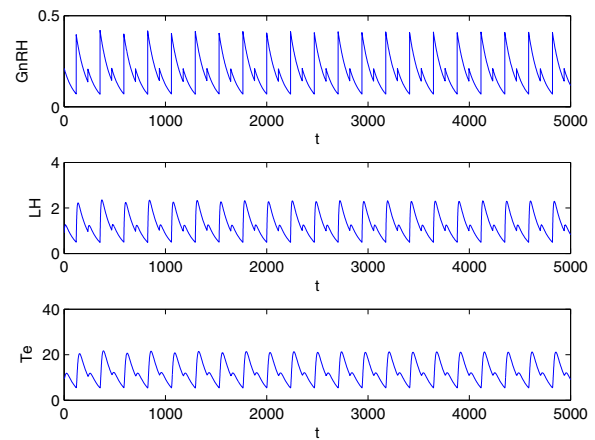


Fig. 10. Example of the temporal variations of concentrations of GnRH, LH and Te for a 2-cycle.  $g_1 = 1.0$ ,  $b_1 = 0.00921$  and  $p = 4$ .

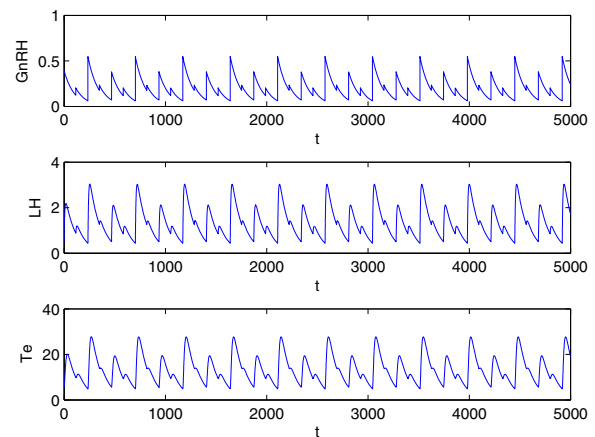


Fig. 11. Temporal variations of concentrations of GnRH, LH and Te for a 4-cycle (see Fig. 8).  $g_1 = 1.0$ ,  $b_1 = 0.01$  and  $p = 4$ .

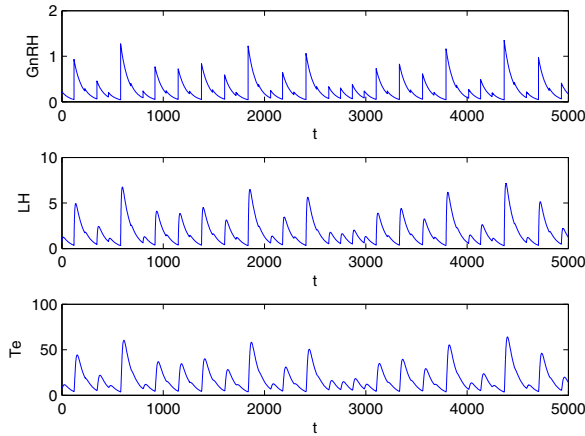


Fig. 12. Temporal variations of concentrations of GnRH, LH and Te for the chaotic dynamics (see Fig. 8).  $g_1 = 1.0$ ,  $b_1 = 0.0128$  and  $p = 4$ .

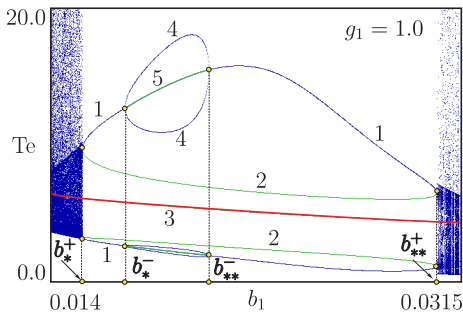


Fig. 13. Magnified part of the bifurcation diagram for  $g_1 = 1.0$  and  $p = 4$  that is outlined by the rectangle in Fig. 8. When the parameter  $b_1$  increases, the 3-cycle undergoes direct and reverse period-doubling bifurcations. Here green lines show the unstable 3-cycle and the red line 3 marks the unstable 1-cycle.  $b_{*+}^+$  and  $b_{*+}^-$  are the saddle-node bifurcation points.  $b_{**}^-$  and  $b_{**}^+$  are the period-doubling bifurcation points.

a union of the sets  $\Pi_{k \cdot 2^{i-1}}$ ,  $i = 1, 2, \dots, \infty$ , where  $\Pi_{k \cdot 2^{i-1}}$  are domains of existence of locally stable  $k \cdot 2^{i-1}$ -cycles ( $i = 1, 2, \dots$ ). Moreover, each domain of stability for  $k \cdot 2^{i-1}$ -cycle is “embedded” into the region of existence for a stable  $k \cdot 2^{i-1}$ -cycle, and delineated by a *closed period-doubling bifurcation curve*.

It is finally demonstrated that the increase in the Hill function order leads to the appearance of a large periodic window that is composed by a finite number of domains of existence for stable cycles, namely  $\Pi_3 \cup \Pi_6$ , with the following peculiarity. The domain of stability for the 3-cycle  $\Pi_3$  is bounded from outside by the saddle-node bifurcation curve  $N_+$  and from inside by the period-doubling bifurcation curve  $N_-$ . The domain of 6-cycle dynamics  $\Pi_6$  is “embedded” into the 3-cycle window  $\Pi_3$ . This implies that the 3-cycle undergoes only two period-doubling bifurcations, first a direct bifurcation, and then a reverse one.

The discovery of chaos in the model is consistent with some published experimental and theoretical results in endocrinology implicating chaos in prominent biological phenomena and provides a simple tool for describing irregularity in hormonal systems. The performed bifurcation analysis

also indicates that higher, but still very moderate, orders of Hill functions in the model give rise to more complex dynamical modes.

#### ACKNOWLEDGMENTS

The authors would like to thank Prof. E. Mosekilde for his careful reading of and constructive suggestions to a first draft of this manuscript. The anonymous reviewers are gratefully acknowledged for their constructive comments.

#### REFERENCES

- [1] J. Murray, *Mathematical Biology, I: An Introduction*. 3rd ed. New York: Springer, 2002.
- [2] L. S. Farhy, “Modeling of oscillations in endocrine networks with feedback,” *Methods in Enzymology*, vol. 384, pp. 54–81, 2004.
- [3] W. S. Evans, L. S. Farhy, and M. L. Johnson, “Biomathematical modeling of pulsatile hormone secretion: a historical perspective,” in *Methods in Enzymology: Computer methods, Volume A*, M. L. Johnson and L. Brand, Eds., 2009, vol. 454, pp. 345–366.
- [4] D. Matthews and P. Hindmarsh, “Hormone pulsatility,” in *Clinical Pediatric Endocrinology*, C. Brook and P. Hindmarsh, Eds. Oxford: Wiley-Blackwell, 2001, pp. 17–26.
- [5] I. Reinecke and P. Deuffhard, “A complex mathematical model of the human menstrual cycle,” *J. Theor. Biol.*, vol. 247, pp. 303–330, 2007.
- [6] S. A. Weinzimer, G. M. Steil, K. L. Swan, J. Dziura, N. Kurtz, and W. V. Tamborlane, “Fully automated closed-loop insulin delivery versus semiautomated hybrid control in pediatric patients with type 1 diabetes using an artificial pancreas,” *Diabetes Care*, vol. 31, no. 5, pp. 934–939, May 2008.
- [7] A. Churilov, A. Medvedev, and A. Shepeljavi, “State observer for continuous oscillating systems with intrinsic pulsatile feedback,” in *IFAC World Congress*, Milano, Italy, September 2011, accepted for presentation.
- [8] G. Enciso and E. Sontag, “On the stability of a model of testosterone dynamics,” *J. Math. Biol.*, vol. 49, pp. 627–634, 2004.
- [9] R. H. Abraham, H. Kocak, and W. R. Smith, “Chaos and intermittency in an endocrine system model,” in *Chaos, Fractals, and Dynamics*, P. Fischer and W. R. Smith, Eds. Marcel Dekker, Inc., 1985, vol. 98, pp. 33–70.
- [10] R. Rössler, F. Götz, and O. Rössler, “Chaos in endocrinology,” *Biophys. J.*, vol. 25, no. 2, p. 216a, 1979.
- [11] C. Sparrow, “Chaos in a three-dimensional single loop feedback system with a piecewise linear feedback function,” *J. Math. Anal. Appl.*, vol. 83, no. 1, pp. 275–291, 1981.
- [12] N. Rasgon, L. Pumphrey, P. Prolo, S. Elman, A. Negro, J. Licinio, and A. Garfinkel, “Emergent oscillations in mathematical model of the human menstrual cycle,” *CNS Spectrums*, vol. 8, no. 11, pp. 805–814, 2003.
- [13] A. Medvedev, A. Churilov, and A. Shepeljavi, “Mathematical models of testosterone regulation,” in *Stochastic Optimization in Informatics*, (In Russian). St. Petersburg State University, 2006, no. 2, pp. 147–158.
- [14] A. Churilov, A. Medvedev, and A. Shepeljavi, “Mathematical model of non-basal testosterone regulation in the male by pulse modulated feedback,” *Automatica*, vol. 45, no. 1, pp. 78–85, 2009.
- [15] G. N. Derry and P. S. Derry, “Characterization of chaotic dynamics in the human menstrual cycle,” *Nonlinear Biomedical Physics*, vol. 4, no. 5, 2010.
- [16] K. Prank, H. Harms, M. Dämmig, G. Brabant, F. Mitschke, and R.-D. Hesch, “Is there low-dimensional chaos in pulsatile secretion of parathyroid hormone in normal human subjects?” *American J. Physiology*, vol. 266, pp. E653–E658, 1994.
- [17] D. M. Keenan, W. Sun, and J. D. Veldhuis, “A stochastic biomathematical models of the male reproduction hormone system,” *SIAM J. Appl. Math.*, vol. 61, no. 3, pp. 934–965, 2000.
- [18] B. J. Blue, B. W. Pickett, E. L. Squir, A. O. McKinnon, T. M. Net, R. P. Amann, and K. A. Shiner, “Effect of pulsatile or continuous administration of gnrh on reproductive function of stallions,” *J. Reprod. Fertil. Suppl.*, vol. 44, pp. 145–154, 1991.
- [19] A. K. Gelig and A. N. Churilov, *Stability and Oscillations of Nonlinear Pulse-modulated Systems*. Boston: Birkhäuser, 1998.
- [20] Y. A. Kuznetsov, *Elements of Applied Bifurcation Theory*. New York: Springer-Verlag, 2004.